3 Neutron Stars

If the core mass exceeds the Chandrasekhar mass limit during a supernova then it collapses until another form of degeneracy pressure kicks in to halt collapse. This pressure is **neutron degeneracy pressure**, which can be obtained from Eq. (7) by the substitution $m_e \to m_n \approx m_p$ in the limit of non-relativistic neutrons:

C & O, Sec. 16.6

$$P \;=\; \frac{(3\pi^2)^{2/3}}{5}\,\frac{\hbar^2}{m_p}\,n_n^{5/3} \quad . \tag{22}$$

The mass-radius relation then becomes

$$M_{ns}\,R_{ns}^3 \;\propto\; \frac{1}{m_p^5}\left(\frac{\hbar^2}{Gm_p}\right)^3 \;\approx\; 0.04M_\odot\left(10^6\mathrm{cm}\right)^3 \quad . \tag{23}$$

This implies that neutron stars should have radii on the order of 10^6 cm.

Plot: Neutron Star Mass-Radius Relation: a Plethora of Models [2]

- It then quickly follows that the escape velocity is

$$v_{esc} \;=\; \sqrt{\frac{2GM_{ns}}{R_{ns}}} \;\sim\; 1.93\times10^{10}\mathrm{cm\ s^{-1}} \;=\; 0.64c \quad . \tag{24}$$

Accordingly,

  * general relativity must be incorporated in calculations involving neutron stars, and so must relativistic equations of state.

  * Moreover, the virial temperatures are relativistic.

  * these ingredients increase the numerical coefficient in Eq. (23) somewhat.

- Since the electron mass does not appear in the expression for the Chandrasekhar mass limit, an equivalent limit for neutron stars must be of the same order of magnitude. Incorporating an appropriate neutron star equation of state, *the upper bound to neutron star masses* is around $3.2M_\odot$.

- Neutron Stars were predicted by Baade and Zwicky in 1932; they were not conclusively discovered until 1967 in the form of pulsars.

Neutron Star Mass-Radius Relations

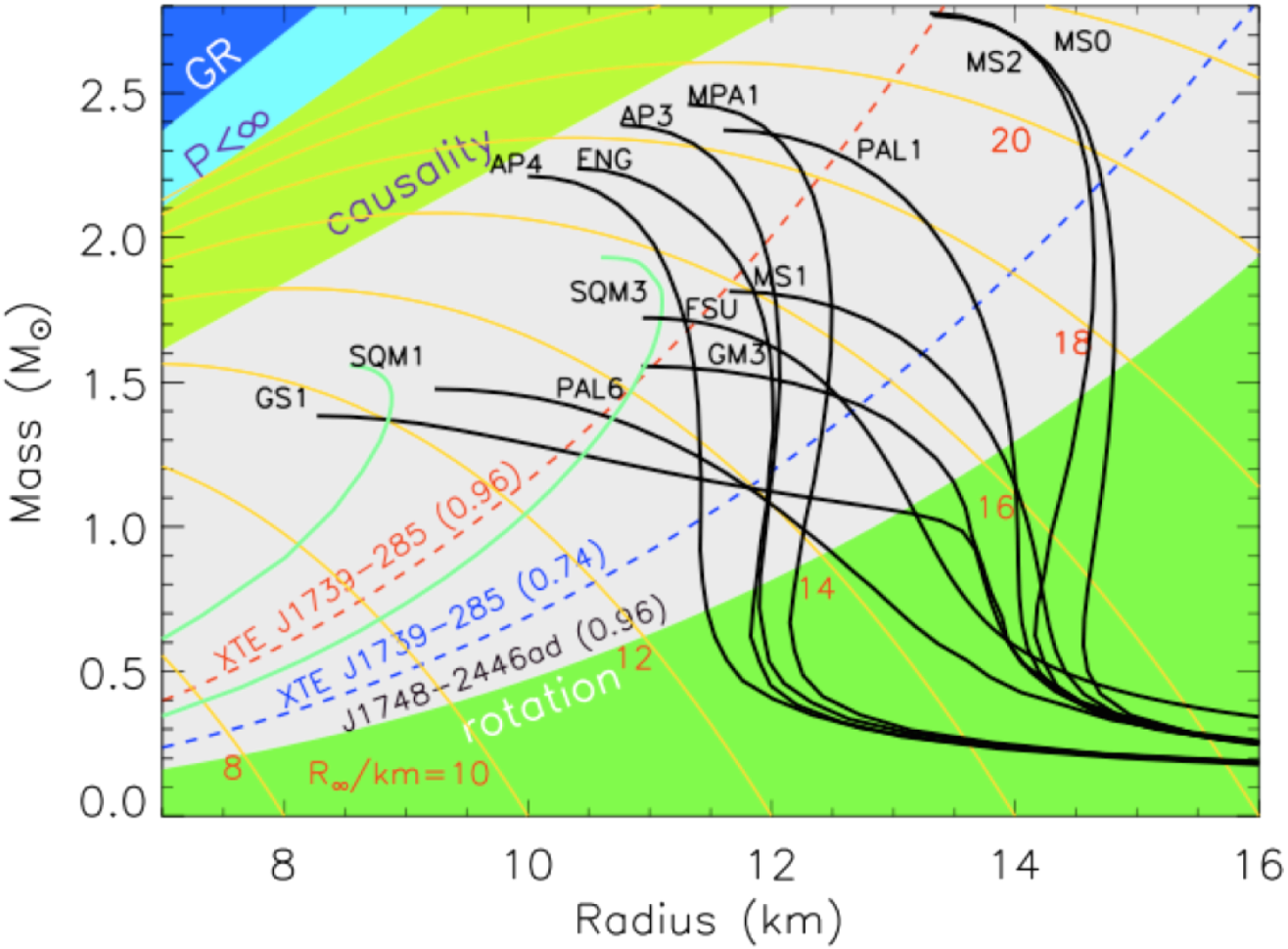

- Various NS interior models in the mass-radius plane; from Lattimer & Prakash (2007, Phys. Rep. **442**, 109).
- Observational constraints for 3 neutron stars are depicted.

• The relativistic temperatures and Fermi energies, and high densities, interior to neutron stars effectively drive the neutron/proton equilibrium

$$p + e^- \;\leftrightarrow\; n + \nu_e \tag{25}$$

to the rapid production of neutrons. This leads to the **neutronization** of elements heavier than iron (e.g. ${}^{66}_{28}Ni$ and ${}^{118}_{36}Kr$), and eventually leads to free neutrons (**neutron drip**) deep in the stellar interior.

Plot: Neutron Star Table

• At what ρ does neutronization occur? Neglecting the neutrino energy, then the energy relation corresponding to Eq. (25) is

$$\frac{m_e c^2}{\sqrt{1 - v_e^2/c^2}} + m_p c^2 \;=\; m_n c^2 \quad , \tag{26}$$

for relativistic electrons, but non-relativistic protons and neutrons. This inverts to the mildly-relativistic result

$$\frac{v_e}{c} \;=\; \left\{ 1 - \left(\frac{m_e}{m_n - m_p} \right)^2 \right\}^{1/2} \;\approx\; 0.919 \quad . \tag{27}$$

Electron degeneracy and Heisenberg's uncertainty principle then yield

$$\frac{v_e}{c} \;=\; \frac{p_e}{m_e c} \;\sim\; \frac{\hbar}{m_e c}\, n_e^{1/3} \;=\; \frac{\hbar}{m_e c} \left(\frac{Z}{A}\, \frac{\rho}{m_p} \right)^{1/3} \quad . \tag{28}$$

Combining and inverting then gives

$$\rho \;\sim\; \frac{A m_p}{Z} \left(\frac{m_e c}{\hbar} \right)^3 \left\{ 1 - \left(\frac{m_e}{m_n - m_p} \right)^2 \right\}^{3/2} \;\sim\; 2.3 \times 10^7 \text{ g cm}^{-3} \quad . \tag{29}$$

At this density, *the Fermi energies of protons and neutrons are non-relativistic*, so that a **stiffer** EOS is operable: $P \propto \rho^{5/3}$.

• The **neutronization phase transition** requires energy, which saps the pressure, and so **softens** the EOS to almost $P \propto \rho^0$. The energy comes from gravitational contraction due to declining pressure support.

Plot: Ideal $n - p - e$ Equation of State

Critical Densities for Onset of Neutronization and GR Instability

	Neutronization Threshold[a] (MeV)	ρ_0 (g cm^{-3})
$^{1}_{1}\mathrm{H} \rightarrow \mathrm{n}$	0.782	1.22×10^{7}
$^{4}_{2}\mathrm{He} \rightarrow {}^{3}_{1}\mathrm{H} + n \rightarrow 4n$	20.596	1.37×10^{11}
$^{12}_{6}\mathrm{C} \rightarrow {}^{12}_{5}\mathrm{B} \rightarrow {}^{12}_{4}\mathrm{Be}$	13.370	3.90×10^{10}
$^{16}_{8}\mathrm{O} \rightarrow {}^{16}_{7}\mathrm{N} \rightarrow {}^{16}_{6}\mathrm{C}$	10.419	1.90×10^{10}
$^{20}_{10}\mathrm{Ne} \rightarrow {}^{20}_{9}\mathrm{F} \rightarrow {}^{20}_{8}\mathrm{O}$	7.026	6.21×10^{9}
$^{24}_{12}\mathrm{Mg} \rightarrow {}^{24}_{11}\mathrm{Na} \rightarrow {}^{24}_{10}\mathrm{Ne}$	5.513	3.16×10^{9}
$^{28}_{14}\mathrm{Si} \rightarrow {}^{28}_{13}\mathrm{Al} \rightarrow {}^{28}_{12}\mathrm{Mg}$	4.643	1.97×10^{9}
$^{32}_{16}\mathrm{S} \rightarrow {}^{32}_{15}\mathrm{P} \rightarrow {}^{32}_{14}\mathrm{Si}$	1.710	1.47×10^{8}
$^{56}_{26}\mathrm{Fe} \rightarrow {}^{56}_{25}\mathrm{Mn} \rightarrow {}^{56}_{24}\mathrm{Cr}$	3.695	1.14×10^{9}

[a] From Wapstra and Bos (1977); the electron rest mass-energy, $m_e c^2 = 0.511$ MeV, has been subtracted off.

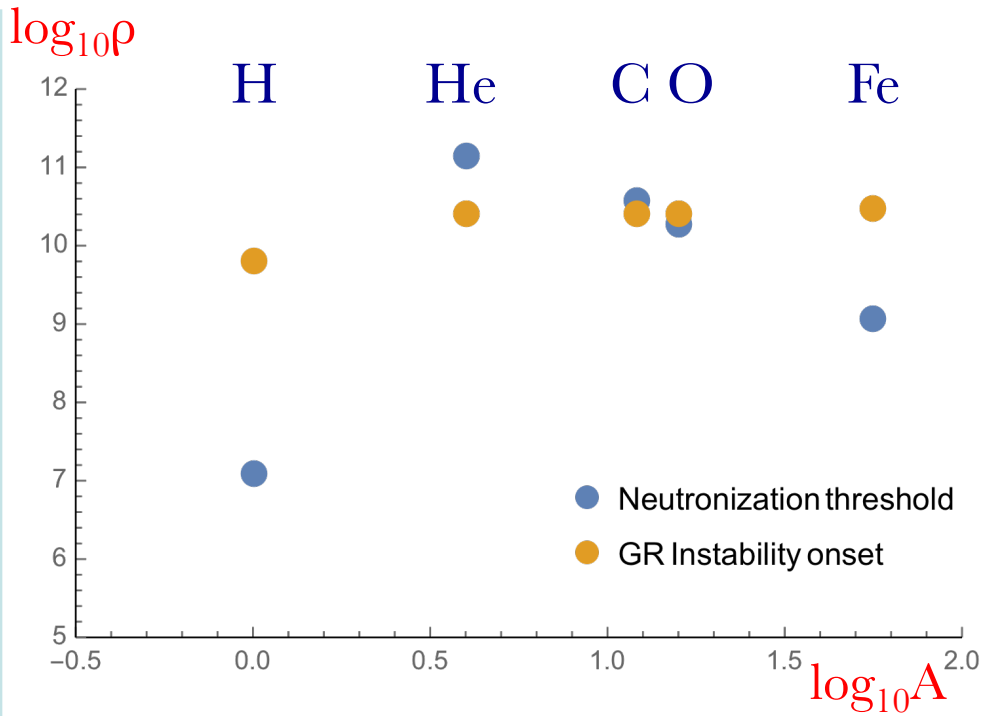

- *Left panel*: Neutronization thresholds and corresponding densities. Positive energy is price of inverse beta decay to increase neutron content => high for He, low for H.
- *Right panel*: Comparison of densities for onset of GR instability and neutronization for different composition white dwarfs. GR limits central density of C+O or He WDs.

Chandrasekhar and Ideal n-p-e$^-$ Equations of State

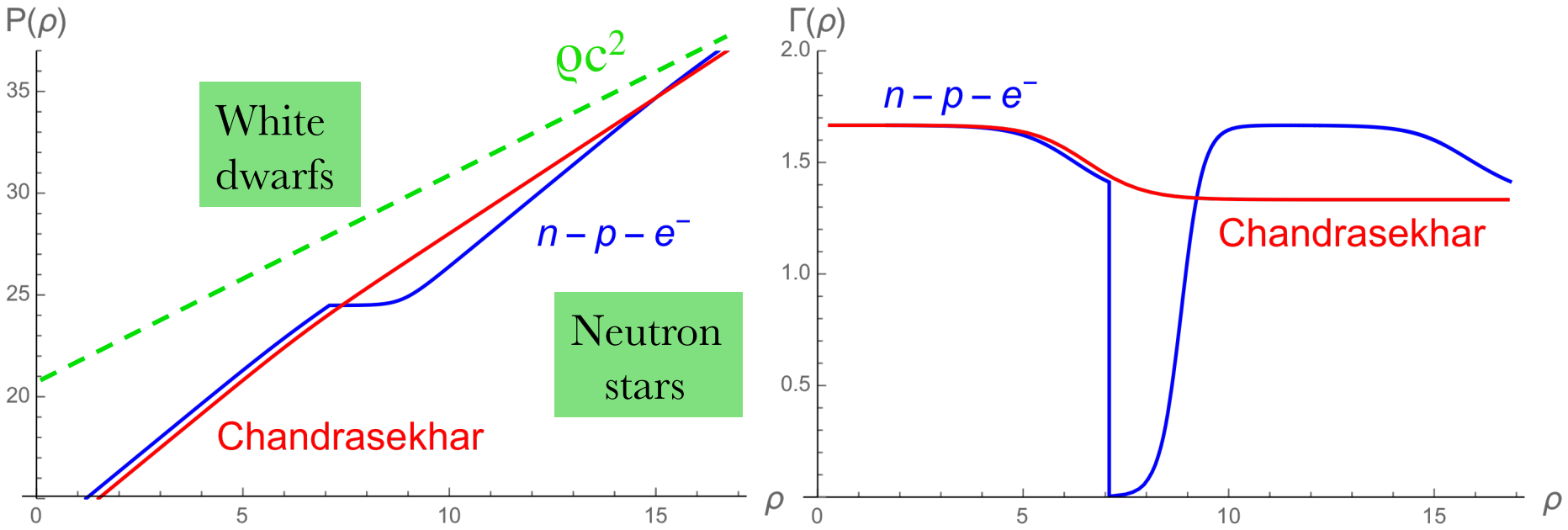

- *Left panel*: Equations of state for the totally degenerate electron Chandrasekhar model and the ideal n-p-e$^-$ equilibrium degenerate gas mixture. The n-p-e$^-$ gas pressure at white dwarf (low) densities includes the proton contribution. The pressure is in dyne cm^{-2} and the density is in g cm^{-3}. *Right panel*: The corresponding adiabatic indices. The drop in index Γ with the onset of neutronization at ~10^7 g cm^{-3} is very prominent.

3.1 Neutron Star Structure

• Neutron decay is suppressed since the high density renders them effectively bound by nuclear forces.

C & O, pp. 580-2

• The neutrons form a superfluid, and at the core, the composition is unknown . . . it may be a pion condensate, or a quark superfluid. The central composition is unknown and is at the core of focal probes of the equation of state (EOS). Different compositions generate different neutrino loss rates.

• The high interior density drives the neutrons to couple as pairs of neutrons, losing Fermionic character and becoming **bosons**. This resembles Cooper-pairing in superconductors.

∗ Since the Pauli exclusion principle does not apply to bosons, all neutron pairs can occupy the ground state. The fluid can therefore lose no energy (e.g. through friction), and so possesses no viscosity – it is a **superfluid**.

∗ whirlpools/vortices in the superfluid will spin forever!

• Residual protons down near the core form bosonic pairs that are **superconducting**, i.e. exhibit zero electrical resistance.

• The EOS can be constrained using surface X-ray diagnostics with Chandra telescope and Rossi X-ray Timing Explorer (RXTE). For example, the gravitational redshift of any spectral features (e.g. Fe lines) would estimate M/R. In practice, this is very rare: it has not arisen yet.

∗ For an ensemble (about 8) of X-ray neutron stars of different ages, the temperature distribution with age can distinguish somewhat between different neutron star models via their predictions of cooling curves.

Plot: Neutron star cooling curves and X-ray temperatures

∗ Rampant neutrino emission from high core density scenarios cools neutron stars too fast, conflicting with observations of middle-aged pulsars.

Neutron Star Cooling Curves

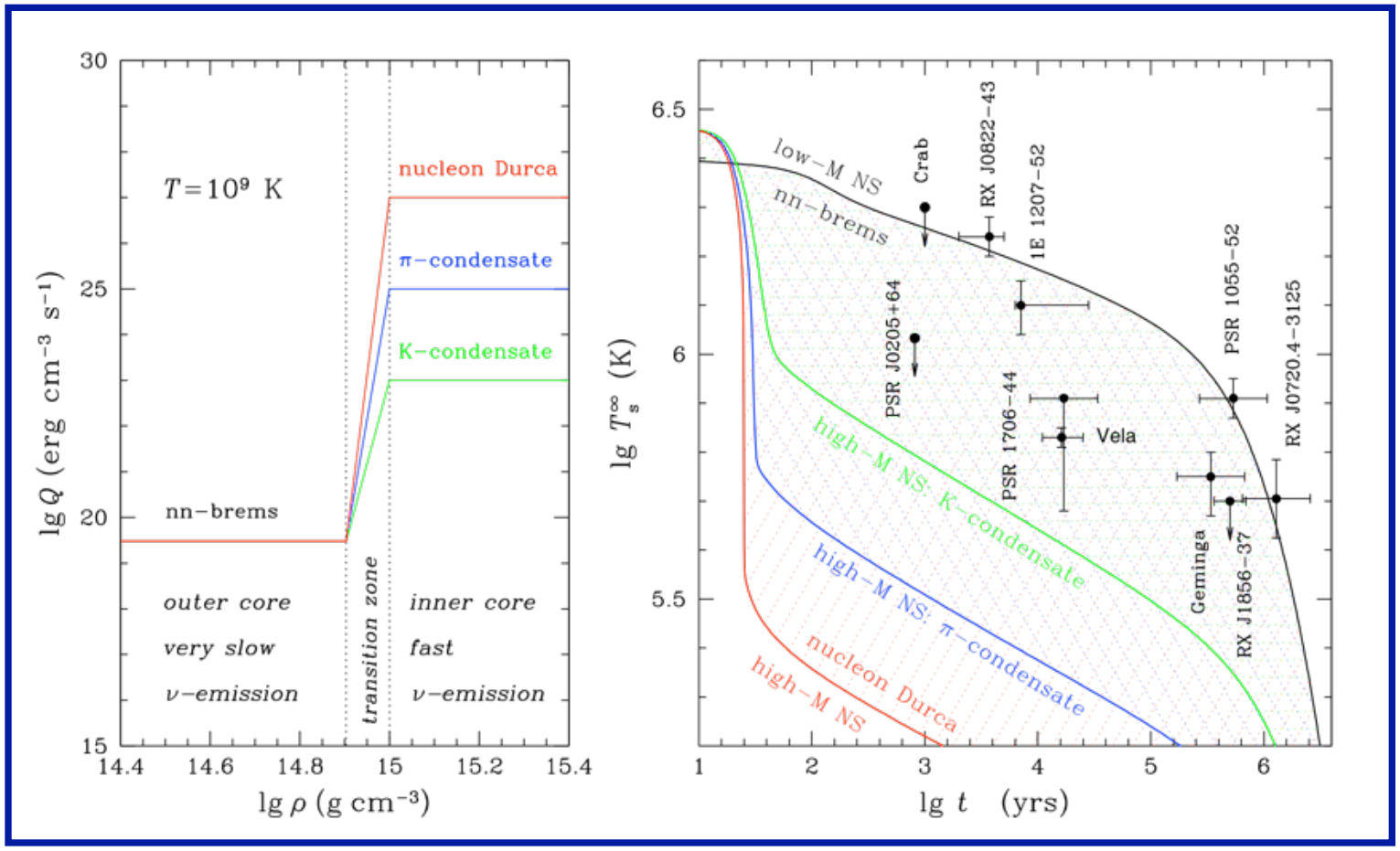

- Exotic neutron star interiors: cooling models summarized in Yakovlev & Pethick (2004, ARAA 42, 169).
- *Left*: Schematic density dependence of the neutrino emissivity in a neutron star core at T = 10^9 K assuming very slow neutrino emission in the outer core and three scenarios for fast emission in the inner core.
- *Right*: Ranges of T^{∞} (single, double and triple hatching) for the three types of fast emission, compared with observations. Each range is limited by the upper cooling curve (low-mass star) and a lower curve (high-mass star).

• Interesting M, R diagnostics can be found via different means. If d is known, the Stefan-Boltzmann law gives L and therefore R if the temperature is measured using Chandra spectroscopy. This can occasional be combined with dynamical estimates of M.

Plot: Dynamical and Other Neutron Star Mass Estimates

• In quasi-edge-on binary systems, gravitational light propagation delays or **Shapiro delay** can probe the mass of the intervening neutron star. A classic example is the millisecond pulsar J1614-2230, illustrating the precision of general relativistic mass determinations.

• Frequencies of **quasi-periodic oscillations** (QPOs) measured by RXTE couple to sound wave/shear wave dynamical timescales R/c_s in surface crustal layers. Inferences of R/c_s can constrain both M and R, and even provide information on the magnetic field strength.

Plot: QPOs in the power spectrum

• The shear wave speed in the crustal lattice can be determined, approximately, by setting the kinetic energy density ρc_s^2 equal to the Coulomb potential energy density Z^2e^2/r^4, where $r \sim (n_i)^{-1/3}$ is the inter-ion spacing, and $n_i = \rho/(Am_p)$. Since $c_s = \sqrt{\partial P/\partial\rho}$, this protocol is essentially equivalent to assigning a Coulomb lattice vibration thermal pressure equal to Z^2e^2/r^4. Thus, $P \propto r^{-4} \propto \rho^{4/3}$, i.e., we have a relativistic EOS. For $\rho \sim 3M_{\rm latt}/[4\pi R^3]$, this then establishes oscillation periods

$$\Pi \;=\; \frac{2\pi R}{c_s} \;\sim\; 2\pi R\,\frac{\rho^{1/2} n_i^{2/3}}{Ze} \;\sim\; \frac{2\pi\, A^{2/3}}{Ze}\,\frac{m_p^{2/3} R^{3/2}}{M_{\rm latt}^{1/6}} \quad , \tag{30}$$

which for $M_{\rm latt} \sim 10^{-2} M_\odot$ and $R \sim 10^6$ cm is of the order of 5×10^{-3} seconds for ${}^{56}_{26}Fe$, consistent with observations of QPOs in the sub-kHz range.

$*$ Period measures of QPOs give $M \sim R^{3\to6}$ in the $M-R$ diagram, orthogonal to model curve predictions.

Observational Bounds on Neutron Star Masses

- Mass constraints of various origins such as dynamical estimates;
- From Lattimer & Prakash (2007, Phys. Rep. **442**, 109);
- No NS have definitive mass measurements above 2 solar masses, but…
- See Demorest et al. (2010, Nature **467**, 1081) for 1.97$M_\odot$ Shapiro delay estimate for binary MSP PSR J1614-2230.

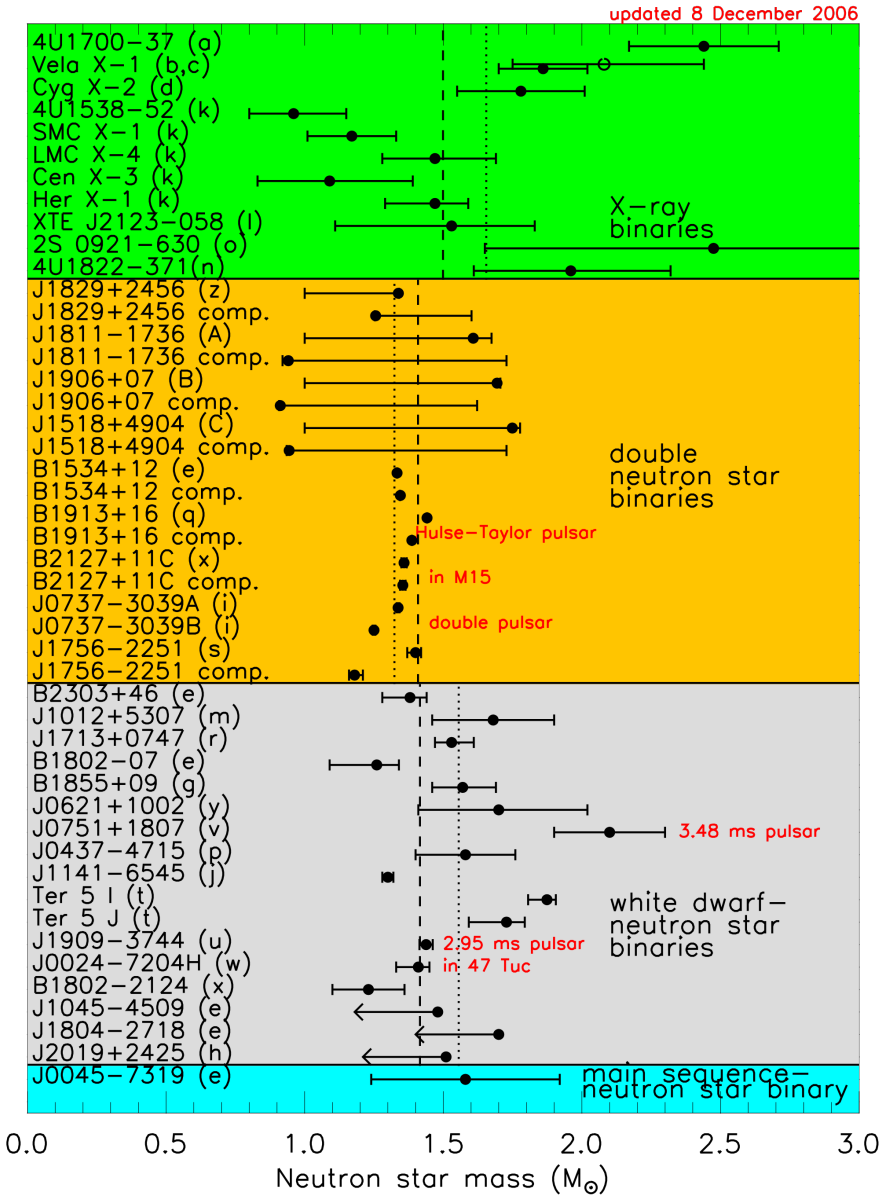

Quasi-Periodic Oscillations in the giant flare for SGR 1900+14 of August 27 1998

- Strohmayer & Watts (ApJ 632, L111, 2005): Rossi X-ray Timing Explorer detection of QPOs at 28Hz, 53 Hz, 84Hz and (main feature) 155Hz.
- Seen in 1 sec interval only (select rotational phase) of pulsed tail following about 1 minute after initial spike.
- Interpreted as torsional global seismic oscillations of crustal ion lattice.
- QPOs seen also in 12/27/04 SGR 1806-20 giant flare tail.